

# $\alpha$ -attractor potentials in loop quantum cosmology

G. L. L. W. Levy<sup>1,\*</sup> and Rudnei O. Ramos<sup>2,†</sup>

<sup>1</sup>*Centro Brasileiro de Pesquisas Físicas, Rua Doutor Xavier Sigaud 150, Urca, 22290-180, Rio de Janeiro, RJ, Brazil*

<sup>2</sup>*Departamento de Física Teórica, Universidade do Estado do Rio de Janeiro, 20550-013 Rio de Janeiro, RJ, Brazil*

We perform in this work an analysis of the background dynamics for  $\alpha$ -attractor models in the context of loop quantum cosmology. Particular attention is given to the determination of the duration of the inflationary phase that is preceded by the quantum bounce in these models. From an analysis of the general predictions for these models, it is shown that we can be able to put constraints in the parameter  $\alpha$  of the potentials and also on the quantum model itself, especially the Barbero-Immirzi parameter. In particular, the constraints on the tensor-to-scalar ratio and spectral tilt of the cosmological perturbations limit the  $\alpha$  parameter of the potentials to values such that  $\alpha_{n=0} \lesssim 10$ ,  $\alpha_{n=1} \lesssim 17$  and  $\alpha_{n=2} \lesssim 67$ , for the  $\alpha$  attractors T, E, and  $n = 2$  models, respectively. Using the constraints on the minimal amount of  $e$ -folds of expansion from the quantum bounce up to the end of inflation leads to the upper bounds for the Barbero-Immirzi parameter for the  $\alpha$ -attractor models studied in this work:  $\gamma_{n=0} \lesssim 51.2$ ,  $\gamma_{n=1} \lesssim 63.4$  and  $\gamma_{n=2} \lesssim 64.2$ , which are obtained when fixing the parameter  $\alpha$  in the potential at the values saturating the upper bounds given above for each model.

## I. INTRODUCTION

Building a theory of quantum gravity is still a challenge. Among the proposals, loop quantum gravity (LQG), which is a background independent and nonperturbative approach for quantizing general relativity (for reviews, see, e.g., Refs. [1–3]) has been widely investigated in the past 30 years or so. Meanwhile, the physical implications of LQG make use of its loop quantization techniques to cosmological models, namely loop quantum cosmology (LQC), which is the symmetry reduced version of LQG [2, 4–9]. In LQC, the quantum effects at the Planck scale are able to produce a bounce that results as a consequence of the repulsive quantum geometrical effects and, hence, effectively resolving the singularity issue of classical general relativity.

Making predictions concerning the inflationary phase that can be preceded by a quantum bounce has attracted quite some interest recently. Interestingly, it has been shown that in LQC that inflation can occur quite naturally, and it is in general a strong attractor when a scalar field is the main ingredient of the energy density. This characteristic of LQC has been confirmed and studied in detail in many recent works [10–15]. These works have shown that in LQC models with a kinetic energy dominated bounce lead to an almost inevitably inflationary phase following the bounce phase.

The discussion of the inflationary phase after the quantum bounce in LQC has been mostly studied following two lines of thoughts on how and when the initial conditions should be taken. One line of thought assumes that the initial conditions can be appropriately taken at the bounce [10–17]. Another school assumes that the appropriate moment to take the initial conditions would be

deep inside the contracting phase before the bounce [18–22]. Both lines of thought lead to the conclusion that inflation is in general a strong attractor; however, in the latter case, when taking initial conditions deep in the contracting phase, it has been further demonstrated that not only inflation is highly probable, but that the duration of inflation itself can be predicted using simple analytical methods as has been shown in Ref. [23]. Having a way of making predictions concerning the inflationary phase is quite important when comparing and contrasting different inflationary models with the observations.

In the present work, we make use of the method developed in Ref. [23] and apply it to the study of the dynamics for the  $\alpha$ -attractor type of potentials [24–26]. We focus in particular on the bouncing dynamics and the subsequent transition (preinflation phase) and inflationary phases following the quantum bounce in LQC. For different values of parameters in these potentials, we verify whether they can produce not only a sufficient number of  $e$ -folds such as to solve the usual big bang problems but also to be compatible with the observational predictions for these types of models, e.g., the tensor-to-scalar ratio and spectral tilt of the scalar perturbations. We note that the preinflationary dynamics in LQC for this class of potentials has also been studied previously in Refs. [15, 27] by adopting the school of thought of taking the initial conditions at the instant of the bounce, as proposed e.g., in Ref. [16]. In this approach, the authors of those references have then checked which initial conditions at the bounce would be able to lead to a sufficient duration of inflation in different  $\alpha$ -attractor models. Here, however, we follow the second line of thought, which argues that the appropriate instant for taking the initial conditions should be in the contracting phase and well before the bounce, as initially proposed in Ref. [18]. As already commented above, this has the additional advantage of making it possible to make precise predictions for what should be the actual duration of inflation and avoids the arbitrariness of the former line of thought, of which initial

\* guslevy9@hotmail.com

† rudnei@uerj.br

condition should one actually take at the bounce instant.

It is important to comment that in this work, like in the previous literature [18–23], we are assuming the vanillalike old LQC description where the deep contracting phase behaves like contracting classical general relativity. But we have to keep in mind that there are other examples of LQC models where the prebounce physics can be much more complicated, like involving a collapsing universe with a large cosmological constant (of Planck order) [28, 29], or that also involves spacetimes that are emergent [30, 31], i.e., with a transition from Minkowski to LQC-FRW. All these models can be considered as motivated from the full theory and can be as well natural extensions of LQC. The results derived in this paper cannot be extended to those other formulations of LQC where the most adequate point of setting the initial conditions might be at the bounce instant and where predictions like the ones we have obtained cannot be derived.

The interest in considering the  $\alpha$ -attractor type of potentials is because they are a well-motivated class of inflationary potentials which are able to lead to universal predictions for large-scale observables that are largely independent of the details of the inflationary potential. Furthermore, they lead to predictions that lie close to the center of current observational bounds on the primordial power spectra [32, 33]. Let us recall that the Starobinsky potential [34], which is shown to fit the current observations quite well, is a particular case of an  $\alpha$ -attractor type of potential.

We have organized this paper as follows. In Sec. II we briefly review the  $\alpha$ -attractor, in particular the T, E, and  $n = 2$  models which are considered in this work. In Sec. III we present the structure of LQC for developing the background dynamics and summarize the methods developed in Ref. [23], which are used in the present study. Our main results are presented in Sec. IV, where we study the background dynamics of the T, E, and  $n = 2$  models, which includes the bouncing, preinflation, and inflation phases and present the predictions that we obtain for these models. We also contrast our results with the previous ones obtained when considering initial conditions taken at the bounce instant. We use these results to constrain the  $\alpha$  parameter of the potentials and also the Barbero-Immirzi parameter when considering it as a free parameter in LQC. Finally, in Sec. V, we present our conclusions. Relevant technical details used in our analysis are also given in the Appendix.

## II. THE $\alpha$ -ATTRACTOR POTENTIALS

In this paper, we consider the following class of  $\alpha$ -

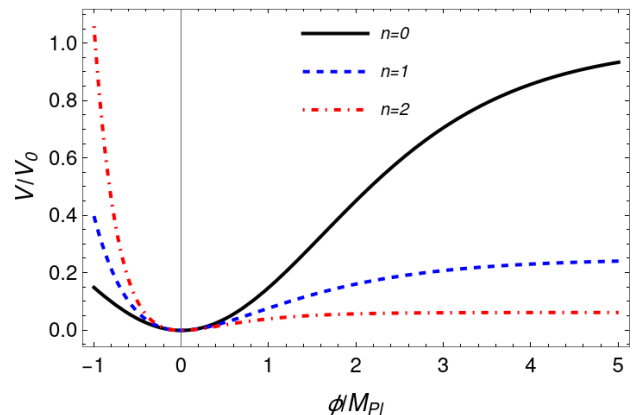


FIG. 1. The  $\alpha$ -attractor potential cases considered in this work. The parameter  $\alpha$  was set to the value  $\alpha = 1$ .

attractor potentials given by [27, 35, 36]

$$V(\phi) = V_0 \frac{\left[ \tanh\left(\frac{\phi}{\sqrt{6\alpha} M_{\text{Pl}}}\right) \right]^2}{\left[ 1 + \tanh\left(\frac{\phi}{\sqrt{6\alpha} M_{\text{Pl}}}\right) \right]^{2n}}, \quad (2.1)$$

where  $M_{\text{Pl}} = m_{\text{Pl}}/\sqrt{8\pi}$  is the reduced Planck mass and  $m_{\text{Pl}} = 1.22 \times 10^{19}$  GeV is the Planck mass, and  $\alpha$  is a dimensionless positive constant. The value of the power  $n$  parametrizes different classes of  $\alpha$ -attractor potentials. We will work with the cases where  $n = 0, 1, 2$ . For instance, for  $n = 0$ , in the literature, this potential is called the T model [25, 37, 38]. The case with  $n = 1$  is known as the E model and it is a generalization of the Starobinsky model [34], which is obtained when  $\alpha = 1$ . In Eq. (2.1), the value of  $V_0$  is the normalization of the potential, which is fixed by the amplitude of the CMB scalar power spectrum for given values of  $n$  and  $\alpha$  (see the Appendix for details). These types of potentials are well motivated for describing dark energy models to explain the late time cosmic acceleration [39], and they are also forms of potentials representing a limiting case of more general modified gravity theories, like the Starobinsky form. For large values of  $\alpha$  the models resemble monomial potentials [25], and if  $\phi \ll M_{\text{Pl}}$  the potentials approach a quadratic form, while for  $\phi \gg M_{\text{Pl}}$  they approach a constant (flattened) form. The three cases we will consider,  $n = 0, 1$ , and  $2$  are shown in Fig. 1 for illustration.

These potentials also represent robust inflationary models when regarding their predictions. When compared with the observational constraints, like with the spectral tilt  $n_s$  and the tensor-to-scalar ratio  $r$ , they are able to fit the data well. For instance, when  $\alpha \ll 1$  and a large number of  $e$ -folds of inflation they lead to [40] (see also the Appendix for details)

$$n_s \simeq 1 - \frac{2}{N_*}, \quad (2.2)$$

and

$$r \simeq \alpha \frac{12}{N_*^2}, \quad (2.3)$$

where  $N_*$  is the number of  $e$ -folds corresponding to the scales crossing the Hubble radius relevant to CMB, typically corresponding to  $N_* = 50 - 60$   $e$ -folds before the end of inflation, depending on the reheating history [41]. In the absence of running, the Planck data measure the spectral index to be [32]

$$n_s = 0.9649 \pm 0.0042, \quad (2.4)$$

while the recent data analysis of the BICEP, Keck Array combined with that from Planck data places the upper bound on the tensor-to-scalar ratio [42],

$$r < 0.036, \quad \text{at } 95\%CL. \quad (2.5)$$

In the Appendix, we show the behavior of both  $r$  and  $n_s$  for the three types of  $\alpha$  attractors studied here and which are valid for any value of  $\alpha$ . It is found that the most constraining condition comes from the tensor-to-scalar ratio, giving the upper bounds on  $\alpha$  obtained, e.g., at the lowest value of  $N_* = 50$ ,

$$\alpha \lesssim \begin{cases} 10, & \text{for } n = 0, \\ 17, & \text{for } n = 1, \\ 67, & \text{for } n = 2. \end{cases} \quad (2.6)$$

### III. BACKGROUND DYNAMICS IN LQC

In LQC, the Friedmann equation is modified by the quantum effects and given by [7, 16]

$$H^2 = \frac{8\pi}{3m_{\text{Pl}}^2} \rho \left( 1 - \frac{\rho}{\rho_{cr}} \right), \quad (3.1)$$

where  $\rho$  is the total energy density and  $\rho_{cr}$  is the critical energy density at which the bounce happens. For  $\rho \ll \rho_{cr}$  we recover general relativity as expected. The critical energy density is given by

$$\rho_{cr} = \frac{\sqrt{3}m_{\text{Pl}}^4}{32\pi^2\gamma^3}, \quad (3.2)$$

and with  $\gamma$  being the Barbero-Immirzi parameter. It is common in the literature of LQC to assume the Barbero-Immirzi parameter as given by the value  $\gamma \simeq 0.2375$ , which is motivated by black hole entropy calculations [43]. However, many authors prefer to consider  $\gamma$  to be a free parameter in quantum gravity theories (see, e.g., Refs. [44–46]). In our analysis, to be performed in the next sections, we will consider both points of view. In particular, when taking  $\gamma$  as a free parameter, we will explore how the type of potentials we are considering in LQC can be made consistent with the observations. This will allow us to put an upper bound in  $\gamma$ .

In this present paper, we work with the dynamics of one scalar field  $\phi$ , the inflaton, with the potential as given by Eq. (2.1) in the three cases mentioned previously, the T model ( $n = 0$ ) the E model ( $n = 1$ ), and the case with  $n = 2$ . In the Friedmann-Lemaître-Robertson-Walker metric, the background evolution for the inflaton is given by

$$\ddot{\phi} + 3H\dot{\phi} + V_{,\phi} = 0, \quad (3.3)$$

where  $V_{,\phi} \equiv dV(\phi)/d\phi$  is the derivative of the inflaton's potential.

As stated in the Introduction I, we follow the background dynamics starting from the contracting phase, well before the bounce, where the initial conditions are set, and follow the dynamics of the inflaton through the bounce, along the postbounce expanding preinflationary phase, the beginning and end of inflation. We follow closely the derivation considered in Ref. [23] for each one of these dynamical phases and for which the detailed analysis was provided. As in the previous references analyzing the dynamics of inflation after the bounce, we will always be assuming that the bounce is dominated by the kinetic energy of the inflaton (which is in fact a natural condition when the initial conditions are taken deep in the contracting phase as shown in Ref. [23]). Since the kinetic energy evolves like a stiff fluid,  $\dot{\phi}^2 \propto 1/a^6$ , it will generically dominate over the potential energy density at the bounce when starting with initial conditions for the inflaton deep in the contracting phase. Below we will summarize the main equations for each one of the phases that will be important for our study.

#### A. Setting the initial conditions in the contracting phase

We set the initial conditions in the classical contracting phase at some instant  $t$  well before the bounce time  $t_B$  and for which the quantum effects are still negligible. In this case, the Hubble parameter can be expressed as

$$H \simeq \frac{1 + \beta}{3(t - t_B)}, \quad (3.4)$$

where  $\beta$  defines here the ratio between potential and kinetic energy densities for the scalar field,  $\beta = V/(\dot{\phi}^2/2)$ .<sup>1</sup> On the other hand, as shown in Ref. [23], the time interval between some instant  $t_\beta$  in the contracting phase for a given value of  $\beta$  and the bounce instant  $t_B$  can also be expressed as

$$t_\beta - t_B = -\frac{1 + \bar{\beta}}{3} \sqrt{\frac{3m_{\text{Pl}}^2 \bar{\beta}}{8\pi(1 + \bar{\beta})V(\phi_\beta)}}, \quad (3.5)$$

<sup>1</sup> Please note that in Ref. [23] the notation  $\alpha$  was used for the ratio between potential and kinetic energy densities for the scalar field. We have changed the notation to avoid confusion with the  $\alpha$  parameter in the potentials considered here.

where  $\phi_\beta \equiv \phi(t_\beta)$  and  $\bar{\beta}$  is taken as the ‘‘average’’ value for  $\beta$ , and we approximate it as a constant within the range  $(0, 1)$  (see Ref. [23] for details). Here, the choice of  $\bar{\beta}$  parametrizes how far in the past we set the initial conditions for the inflaton field. Once the potential  $V(\phi)$  is specified,  $\phi_\beta$  is obtained by the solution of

$$\frac{V(\phi_\beta)}{V'(\phi_\beta)} = \frac{\sqrt{1+\bar{\beta}}}{4\sqrt{3\pi}} m_{\text{Pl}}. \quad (3.6)$$

As shown in Ref. [23] (for a similar earlier prescription, see also Ref. [16]), there is one value of  $\bar{\beta}$  that can be fixed once and for all for all potentials, given by  $\bar{\beta} = 1/3$  and which is the value we will be using throughout our analysis. This value of  $\bar{\beta} = 1/3$  was determined in Ref. [23] by comparing the numerical results for the number of  $e$ -folds of inflation for different potentials obtained by a statistical analysis performed in Ref. [22], which considered a large number of random initial conditions deep in the contracting phase and each one of those initial conditions evolved up to the end of inflation. This allowed for a probability distribution function for each potential to be obtained, from which statistical predictions for the number of  $e$ -folds were derived. As shown in Ref. [23], the comparison of those numerical results with the analytical ones obtained using  $\bar{\beta} = 1/3$  agree quite well, with overall differences which are less than 5%.

### B. The bounce phase

The solution  $\phi_\beta$  can be connected with the valid one around the bounce phase. As at the bounce phase we generically expect  $\dot{\phi}^2/2 \gg V$ , thus leading to

$$\ddot{\phi} + 3H\dot{\phi} \approx 0, \quad (3.7)$$

and we can solve Eq. (3.7) when using (3.1), with the initial condition  $\phi(t_B) = \phi_B$ , to obtain [10]

$$\phi(t) = \phi_B \pm \frac{m_{\text{Pl}}}{2\sqrt{3\pi}} \operatorname{arcsinh} \left[ \sqrt{\frac{24\pi\rho_{\text{cr}}}{m_{\text{Pl}}^4}} \frac{(t - t_B)}{t_{\text{Pl}}} \right]. \quad (3.8)$$

As shown in Ref. [23], the solution given by Eq. (3.8) holds well even deep in the contracting phase. This allows one to determine  $\phi_B$  once  $\phi_\beta$  is obtained.

### C. The postbounce preinflationary phase

After the bounce, in the expanding phase the kinetic energy of the inflaton dilutes faster than its po-

tential energy. We denote this phase, that lasts from the bounce instant  $t_B$  up to the transition point  $t_{tr}$ , where the potential energy equates to the kinetic energy (i.e.,  $\dot{\phi}^2(t_{tr})/2 = V(\phi(t_{tr}))$ , or  $w = 0$ ), as the postbounce preinflationary phase. The inflaton’s amplitude in the transition time is

$$\phi(t_{tr}) = \phi_B + \frac{m_{\text{Pl}}}{2\sqrt{3\pi}} \operatorname{arcsinh} \left[ \sqrt{\frac{24\pi\rho_{\text{cr}}}{m_{\text{Pl}}^4}} \frac{(t_{tr} - t_B)}{t_{\text{Pl}}} \right], \quad (3.9)$$

and the time at this transition point  $t_{tr}$  is determined by solving

$$\dot{\phi}(t_{tr}) = \sqrt{2V(\phi(t_{tr}))}, \quad (3.10)$$

where we choose the convention of positive sign in both Eqs. (3.8) and (3.10) as explained in Ref. [23]. We note that explicit analytical expressions for both  $t_{tr} - t_B$  and  $\phi(t_{tr})$  can be obtained from these equations by approximating them by considering that  $t_{tr} - t_B \gg t_{\text{Pl}}$  as shown in Ref. [10]. However, these expressions are in general too complicated, and since Eq. (3.10) is valid for any potential, it is simpler just to directly solve it numerically, as we do here.

### D. The inflationary phase

Soon after the transition phase, inflation starts. The instant of the start of the accelerating inflationary regime,  $t_i$ , is given when  $w = -1/3$ , i.e., when  $\dot{\phi}_i^2 = V(\phi_i)$ . The time interval between the transition phase and the beginning of inflation has been shown to be very short [10], lasting much less than one  $e$ -fold and can be neglected. This allows us to obtain  $\phi_i \equiv \phi(t_i)$  as

$$\phi_i \simeq \phi_{tr} + \dot{\phi}_{tr} t_{tr} \ln \frac{t_i}{t_{tr}}. \quad (3.11)$$

Finally, from the slow-roll coefficient  $\epsilon_V$ ,

$$\epsilon_V = \frac{m_{\text{Pl}}^2}{16\pi} \left( \frac{V'}{V} \right)^2, \quad (3.12)$$

we determine the inflation amplitude at the end of inflation,  $\phi_{\text{end}}$ , by setting  $\epsilon_V = 1$ . For the  $\alpha$ -attractor class of potentials considered here, Eq. (2.1), we obtain that

$$\phi_{\text{end}} = 4\sqrt{3\pi\alpha} m_{\text{Pl}} \operatorname{arccoth} \left[ \frac{1}{2} \left( n + \sqrt{3\alpha} + \sqrt{(-2+n)^2 + 2n\sqrt{3\alpha} + 3\alpha} \right) \right]. \quad (3.13)$$

The total number of  $e$ -folds of inflation is then given by

$$N_{\text{infl}} \approx \frac{8\pi}{m_{\text{Pl}}^2} \int_{\phi_{\text{end}}}^{\phi_i} \frac{V}{V'} d\phi. \quad (3.14)$$

#### IV. RESULTS

Let us now present our results obtained from the analysis of the  $\alpha$ -attractor models considered here. As a preliminary analysis, we consider the case where the initial conditions are set at the bounce instant  $t_B$ , according to the philosophy adopted in Refs. [15, 27] in the study using these types of inflaton potential. This will allow us to confront how well the analytical results produced for these potentials perform when compared with the numerical ones, obtained by a direct numerical solution of the background evolution equation for the inflaton, Eq. (3.3), with the modified Friedmann equation (3.1) in LQC. Note that in this case, we set arbitrary values for the inflaton amplitude  $\phi_B$  at the bounce, but still subjected to the condition that at the bounce the kinetic energy would dominate over the potential energy of the inflaton,  $\dot{\phi}_B^2/2 \gg V(\phi_B)$ . After this preliminary study, we will follow the philosophy that the initial conditions should be taken deep in the contracting phase and follow the dynamics from this point on up to the end of inflation. In this case, we follow the methodology presented in Ref. [23] and summarized in the previous section. In these first two analyses, we work with a Barbero-Immirzi parameter that is fixed at the value  $\gamma = 0.2375$  as motivated by black hole thermodynamic studies. Finally, we will let  $\gamma$  vary and determine how the dynamics of the  $\alpha$ -attractor models can lead to constraints on its value when confronted with the observations.

##### A. Initial conditions set at the bounce

By setting the initial conditions at the bounce, we fix  $\phi_B$  and then using Eqs. (3.8), (3.10), (3.11), and (3.13), we evaluate the inflaton's amplitude at the transition point, at the beginning and at the end of inflation. We denote these results as being the analytical ones. The assumed value for  $\phi_B$  is such that the number of  $e$ -folds produced are not too large and, thus, we can better control the numerical solution as far as precision and time of evaluation are concerned. Then, the numerical results are obtained by using the same value for  $\phi_B$ , but numerically evolving Eq. (3.3) with the Friedmann equation (3.1) and obtained in Ref. [27]. We also choose the initial conditions such that the evolution is always at the flatter region of the  $\alpha$ -attractor models (see Fig. 1), i.e.,  $\phi_B > 0$  and  $\dot{\phi}_B > 0$ . The results for each of the corresponding phases and the number of  $e$ -folds for the inflationary phase for the T-model ( $n = 0$ ), E-model ( $n = 1$ ), and for the  $n = 2$   $\alpha$ -attractor models are shown in Table I. To

obtain these results, we have considered the parameter value  $\alpha$  for each model as set to  $\alpha_{n=0} = 5$ ,  $\alpha_{n=1} = 5$ , and  $\alpha_{n=2} = 30$ , whose values are consistent with the ones given by the upper bounds given in Eq. (2.6). The normalization  $V_0$  for each potential is computed according to the Appendix and always at the  $N_* = 50$  value for definiteness.

In Table I, the result for  $N_{\text{infl}}$  in parentheses for the numerical results indicates the inflationary number of  $e$ -folds computed according to the slow-roll approximation, Eq. (3.14), whose formula we also used when estimating the analytical results. The number of  $e$ -folds without the parentheses is obtained when we follow the exact slow-roll coefficient  $\epsilon_H = -\dot{H}/H^2$  when it first becomes equal to 1 in the expanding phase after the bounce (e.g.,  $w_\phi = -1/3$ ) and when it gets equal to 1 again later at the end of inflation. As noticed by the results shown in Table I, the largest differences come from the obtained number of  $e$ -folds in each method. The slow-roll formula, Eq. (3.14), produces results with a difference between the analytic and numerical results that is of order of 10%.

##### B. Initial conditions set in the far past in the contracting phase

We now consider the line of thought that the appropriate moment to take the initial conditions should be deep inside the contracting phase before the bounce [18–22]. We follow the evolution of the inflaton field from deep inside the contracting phase, before the bounce, until up to the end of inflation, according to the method explained in Ref. [23] and summarized in the previous section, Sec III. As shown in Ref. [23], provided the initial conditions are set sufficiently far back in the contracting phase, the bounce will always be dominated by the kinetic energy of the inflaton, which always grows much faster than the energy density in the potential of the inflaton. This then allows one to uniquely compute and determine the evolution of the inflaton up to the end of inflation. In particular, the total number of  $e$ -folds of inflation  $N_{\text{infl}}$  becomes a predicted quantity for a given potential. The obtained results for the  $\alpha$ -attractor potentials considered in this work are shown in Table II. Here, we once again fixed the Barbero-Immirzi parameter at the value  $\gamma = 0.2375$  and considered the values for the parameter  $\alpha$  as given in the previous analysis above,  $\alpha_{n=0} = 5$ ,  $\alpha_{n=1} = 5$ , and  $\alpha_{n=2} = 30$ . The cases of varying  $\alpha$  and  $\gamma$  will also be considered below.

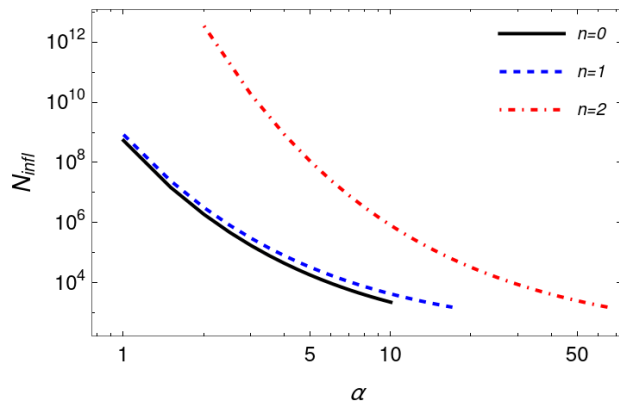
In Fig. 2, we still consider the Barbero-Immirzi parameter fixed at  $\gamma = 0.2375$ , but study how the results for the number of  $e$ -folds of inflation  $N_{\text{infl}}$  changes by varying the parameter  $\alpha$  for each model. The maximum value for  $\alpha$  for each model is taken as given by the upper bounds given in Eq. (2.6) such that the  $\alpha$ -attractor models are consistent with the observations.

TABLE I. Comparison between the numeric and analytic solution for T ( $n = 0$ ), E ( $n = 1$ ), and  $n = 2$   $\alpha$ -attractor models.

Model	$\phi_B/m_{\text{Pl}}$	$\phi_{\text{tr}}/m_{\text{Pl}}$	$\phi_i/m_{\text{Pl}}$	$N_{\text{infl}}$
$n = 0$ (numeric)	0.10	2.35	2.39	178.3 (144.3)
$n = 0$ (analytic)	0.10	2.38	2.44	158.5
$n = 1$ (numeric)	0.10	2.37	2.41	355.1 (287.0)
$n = 1$ (analytic)	0.10	2.40	2.46	316.2
$n = 2$ (numeric)	0.10	2.34	2.38	210.4 (172.1)
$n = 2$ (analytic)	0.10	2.38	2.43	162.7

TABLE II. The predicted results for  $\phi_B$ ,  $\phi_{\text{tr}}$ ,  $\phi_i/m_{\text{Pl}}$ , and  $N_{\text{infl}}$  for the three forms of the  $\alpha$ -attractor models.

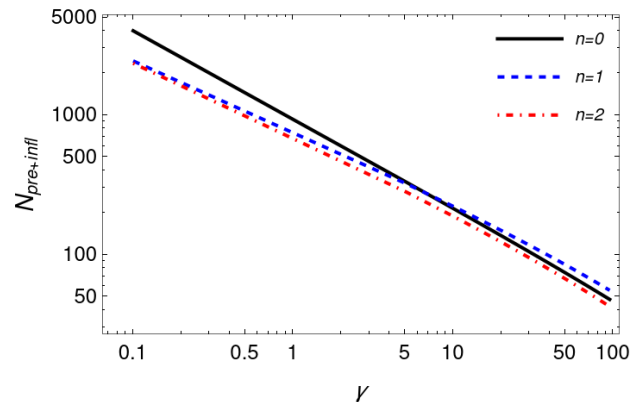
Models	$\phi_B/m_{\text{Pl}}$	$\phi_{\text{tr}}/m_{\text{Pl}}$	$\phi_i/m_{\text{Pl}}$	$N_{\text{infl}}$
T-model ( $\alpha = 5$ )	2.69	4.97	5.02	$1.84 \times 10^4$
E-model ( $\alpha = 5$ )	2.62	4.92	4.97	$3.36 \times 10^4$
$n = 2$ model ( $\alpha = 30$ )	2.62	4.89	4.95	$8.87 \times 10^3$

FIG. 2. Number of inflationary  $e$ -folds  $N_{\text{infl}}$  for the  $\alpha$ -attractor potentials as a function of the  $\alpha$  parameter. The Barbero-Immirzi parameter is kept at the value  $\gamma = 0.2375$ . The upper values of  $\alpha$  considered for each model follow from Eq. (2.6).

We note from the results shown in Fig. 2 that the smaller the parameter  $\alpha$  is, the larger the number of  $e$ -folds predicted for each model is. This is consistent with the fact that the smaller is  $\alpha$ , the region of the potentials where inflation begins gets flatter, thus generically leading to a larger number of  $e$ -folds of inflation.

### C. Varying the Barbero-Immirzi parameter

Finally, we now consider the effect of varying the Barbero-Immirzi parameter  $\gamma$ . As seen from the results of Fig. 2, small values of  $\alpha$  will always lead to a larger number of  $e$ -folds. Since the number of  $e$ -folds of inflation has necessarily a lower bound set by the requirement of inflation to solve the usual flatness and horizon problems

FIG. 3. Number of  $e$ -folds of evolution from the bounce up to the end of inflation,  $N_{\text{pre+infl}}$  as a function of the Barbero-Immirzi parameter  $\gamma$ . The parameter  $\alpha$  in the potential is kept fixed at the values saturating the bound given by Eq. (2.6) for each model.

of the hot big bang model, we fix  $\alpha$  in each model such as to saturate the upper bound given by Eq. (2.6). The corresponding results are given in Fig. 3.

Note that in Fig. 3 we show the total number of  $e$ -folds from the bounce up to the end of inflation,  $N_{\text{pre+infl}}$ , i.e., we also consider the duration of the preinflationary post-bounce phase. Here, we can take advantage of the fact that the linear perturbations in LQC are known analytically [10]. In particular, from the knowledge of the perturbation spectra in LQC, it has been shown in Ref. [23] that there is an upper bound for the Barbero-Immirzi parameter determined by the condition on  $N_{\text{pre+infl}}$ ,

$$N_{\text{pre+infl}} \gtrsim 79 - \frac{3}{2} \ln(\gamma). \quad (4.1)$$

This allows us to find that the consistency of the perturbation spectra in LQC for the  $\alpha$ -attractor models considered here with the observations, when fixing the pa-

parameter  $\alpha$  in the potential at the values saturating the bound given by Eq. (2.6) for each model, then leads to the following upper bounds on  $\gamma$ :

$$\gamma \lesssim \begin{cases} 51.2, & \text{for } n = 0 \text{ and } \alpha = 10, \\ 63.4, & \text{for } n = 1 \text{ and } \alpha = 17, \\ 64.2, & \text{for } n = 2 \text{ and } \alpha = 67, \end{cases} \quad (4.2)$$

such that larger values of  $\gamma$  than these bounds would violate Eq. (4.1).

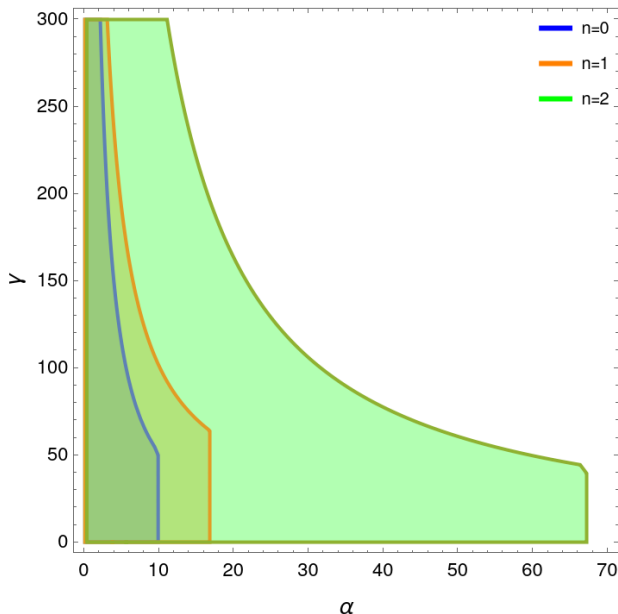


FIG. 4. The allowed region in the  $\alpha$  and  $\gamma$  parameter plane for the three cases of  $\alpha$ -attractor potential studied here.

For completeness, in Fig. 4 we show the region of parameters  $\alpha$  and  $\gamma$  consistent with both Eq. (4.1) and on the allowed range for the tensor-to-scalar ratio and spectral tilt (see the Appendix) for the three cases of  $\alpha$ -attractor potential studied here. Note that the larger the value of  $n$  is in the  $\alpha$ -attractor potential, the allowed region extends more and more toward the right in Fig. 4. We can also understand the allowed region shown in Fig. 4 by noticing that for values of  $\gamma$  smaller than the upper bounds given by Eq. (4.2), the number of  $e$ -folds is sufficiently large to satisfy the condition set by Eq. (4.1). In this case, the upper bound in the tensor-to-scalar ratio, Eq. (2.5), is dominant and independent of  $\gamma$ . But as  $\gamma$  increases, then the number of  $e$ -folds tends to decrease according to Eq. (4.1). Then, the  $\alpha$  parameter has to be changed to compensate, leading to a flatter potential (allowing for a larger number of  $e$ -folds).

Before closing this section, it is worth commenting that the result given by Eq. (4.1) was derived in the context of the dressed metric approach for the perturbations in LQC [47]. Equation (4.1) is obtained using that in the

perturbations derived in the dressed metric approach the spectrum receives corrections that depend on a characteristic scale  $k_B$  at the bounce, which is the shortest scale (or more precisely, the largest wave number  $k_B$  that feels the spacetime curvature during the bounce). The correction in the power spectrum can be seen as a modification of the Bunch-Davis vacuum for the quantum fluctuations due to mode excitations as a consequence of the quantum bounce in LQC. The modification of the power spectrum is constrained by the observations, which then put a constraint on  $k_B$  [10, 48],  $k_B < 1.9 \times 10^{-4} \text{ Mpc}^{-1}$  at  $1\sigma$ . Since  $k_B$  and the total number of  $e$ -folds  $N_T$  from the bounce until today are related,

$$k_B \equiv \frac{\sqrt{8\pi\rho_{\text{cr}}}a_B}{m_{\text{Pl}}} = m_{\text{Pl}} \left( \frac{\sqrt{3}}{4\pi\gamma^3} \right)^{1/2} e^{-N_T}, \quad (4.3)$$

we can then derive the condition on  $N_{\text{pre+infl}}$  as given by Eq. (4.1) and detailed in Ref. [23].

Even though Eq. (4.1) was derived in the context of the dressed metric quantization approach, the result is also qualitatively similar when derived in the hybrid quantization approach. In the hybrid quantization approach [49], there is a similar enhancement of the power spectrum like in the dressed case. The characteristic scale is now  $k_H = k_B/\sqrt{3}$ , and the constraint from the observations now leads to [50]  $k_H < 4.1 \times 10^{-4} \text{ Mpc}^{-1}$ . Overall, in this case the resulting upper bound in the number of  $e$ -folds from the bounce until the end of inflation turns out to be similar to Eq. (4.1). Thus, our results can as well be applied to the case of the hybrid quantization approach.<sup>2</sup>

## V. CONCLUSIONS

In this paper, we have revisited some of the results concerning a class of  $\alpha$ -attractor potentials in the context of LQC. We have considered the background evolution for these types of potentials by following the dynamics when setting the initial conditions at the bounce and also in the deep contracting phase before the bounce. The latter case has been claimed in the recent literature to be the correct point where the initial conditions should be set. It has been shown in several references [18–22] that in this case the inflationary evolution can be predicted. By taking advantage of the results obtained in Ref. [23], we have studied the dynamics of the  $\alpha$ -attractor models when varying the potential parameter  $\alpha$  and also the Barbero-Immirzi parameter  $\gamma$ . By contrasting the results

<sup>2</sup> It is also worth mentioning that the bounds on either  $k_B$  or  $k_H$  are a result of the deviations from the standard  $\Lambda\text{CDM}$  model due to the quantum bounce and that appear at infrared scales in the CMB. These deviations of the power spectrum with respect to the standard model and which depend on the quantization approach used in LQC, have been studied in several papers [29, 51–54].

with the observations, we were able to put constraints on both of these parameters. In particular, the tensor-to-scalar ratio imposes the upper bounds in the  $\alpha$  parameter as being,  $\alpha_{n=0} \lesssim 10$ ,  $\alpha_{n=1} \lesssim 17$ , and  $\alpha_{n=2} \lesssim 67$ , for the  $\alpha$ -attractors T, E, and  $n = 2$  models, respectively.

Our results have also shown that by decreasing the  $\alpha$  parameter, the number of  $e$ -folds predicted for each model in LQC increases. Likewise, the lower the value for the Barbero-Immirzi parameter is, the larger also is the number of  $e$ -folds of inflation. Then, by a previous general bound determined in Ref. [23] and set on the total duration of the preinflationary postbounce and later inflationary phases in LQC, we were able to find the further upper bounds for the Barbero-Immirzi parameter for the  $\alpha$ -attractor models, when fixing the parameter  $\alpha$  in the potential at the values saturating the upper bounds given above for each model:  $\gamma_{n=0} \lesssim 51.2$ ,  $\gamma_{n=1} \lesssim 63.4$ , and  $\gamma_{n=2} \lesssim 64.2$ . Our results show that when we combine constraints on the observables and predictions about the duration of inflation in LQC, general bounds can be set on the  $\alpha$ -attractor potentials and also on the Barbero-Immirzi parameter.

In general, for most of the parameter region for the allowed values for  $\alpha$  and for the Barbero-Immirzi parameter, our results predict a large number of  $e$ -folds for the  $\alpha$ -attractor potentials studied here. A large number of  $e$ -folds is typically associated with the so-called trans-Planckian problem [55, 56] (for a more recent discussion, made in connection with the swampland conjectures of quantum gravity, see, e.g., [57, 58]). Inflation models with a large number of  $e$ -folds are also associated with the presence of eternal inflation [59], which can be considered typical for potentials with very flat plateaus, like the ones considered here. Possible observational consequences of the trans-Planckian problem in the context of LQC have also been recently considered in Ref. [54], indicating that the results are very much model dependent. Independent of the formal issues related to the trans-Planckian problem, we recall that there are some models that in fact require a large number of  $e$ -folds, like in the relaxation inflation model [60], in stochastic axion scenarios [61–63], and in some quintessence models [64, 65]. We believe that delving into the issues that the prediction of a large number of  $e$ -folds in the models studied here might present is beyond the scope of our work, but this is certainly something worth exploring in the future.

## ACKNOWLEDGEMENTS

G.L.L.W.L. acknowledges financial support of the Coordenação de Aperfeiçoamento de Pessoal de Nível Superior (CAPES) - Finance code 001. R.O.R. acknowledges financial support by research grants from Conselho Nacional de Desenvolvimento Científico e Tecnológico (CNPq), Grant No. 307286/2021-5, and from Fundação Carlos Chagas Filho de Amparo à Pesquisa do Estado do Rio de Janeiro (FAPERJ), Grant No. E-

26/201.150/2021.

## APPENDIX

The normalization  $V_0$  of the inflaton potential is fixed by the amplitude of the CMB primordial scalar of curvature power spectrum  $\Delta_{\mathcal{R}}$ , given by [66]

$$\Delta_{\mathcal{R}} = \left( \frac{H_*^2}{2\pi\dot{\phi}_*} \right)^2, \quad (5.1)$$

where a subindex  $*$  means that the quantities are evaluated at the Hubble radius crossing  $k_*$  ( $k_* = a_* H_*$ ), which typically happens around  $N_* \sim 50 - 60$   $e$ -folds before the end of inflation. From the Planck Collaboration [67],  $\ln(10^{10}\Delta_{\mathcal{R}}) \simeq 3.047$  (TT,TE,EE-lowE+lensing+BAO 68% limits). During the slow-roll regime of inflation, we have  $H^2 \simeq 8\pi V/(3m_{\text{Pl}}^2)$  and  $\dot{\phi} \simeq -V_{,\phi}/(3H)$ , which then gives for Eq. (5.1) the result

$$\Delta_{\mathcal{R}} \simeq \frac{128\pi}{3} \frac{V_*^3}{m_{\text{Pl}}^6 V_{,\phi_*}^2}. \quad (5.2)$$

By fixing  $N_*$ , we can determine  $\phi_*$  by solving the number of  $e$ -folds equation,

$$N_* = \frac{8\pi}{m_{\text{Pl}}^2} \int_{\phi_{\text{end}}}^{\phi_*} \frac{V}{V'} d\phi. \quad (5.3)$$

For the  $\alpha$ -attractor class of potentials considered here, Eq. (2.1),  $\phi_{\text{end}}$  is given by Eq. (3.13) and  $N_*$  is found to be given by

$$\begin{aligned} N_* = & \frac{3\alpha}{4n(n-2)^2} \{2b(n-2)^2 - (n-2)[n(e^{2b} - y_*) \\ & + (n-2)\ln(y_*)] - 4(n-1)(\ln[e^{2b}(n-2) + n] \\ & - \ln(n + 2y_* - ny_*))\}, \end{aligned} \quad (5.4)$$

where we have defined

$$y_* = e^{\frac{2}{3\alpha} \frac{\phi_*}{m_{\text{Pl}}}}, \quad (5.5)$$

$$b = \text{arccoth}(a_n), \quad (5.6)$$

and

$$a_n = \frac{1}{2} \left[ n + \sqrt{3\alpha} + \sqrt{(n-2)^2 + 2n\sqrt{3\alpha} + 3\alpha} \right]. \quad (5.7)$$

From Eq. (5.4), we then find that for the T model ( $n = 0$ )

$$\phi_*^{n=0} = \frac{m_{\text{Pl}}}{4} \sqrt{\frac{3\alpha}{\pi}} \text{ArcCosh} \left[ \frac{4N_*}{3\alpha} - \frac{1+a_0^2}{1-a_0^2} \right], \quad (5.8)$$



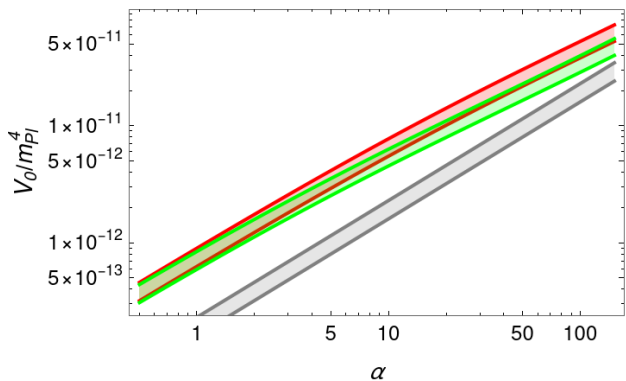


FIG. 5. The normalization  $V_0$  for the  $\alpha$ -attractor potential models considered in this work. The gray, green, and red curves and respective regions are for the T-model ( $n = 0$ ), E-model ( $n = 1$ ) and  $n = 2$   $\alpha$ -attractor models, respectively. They are obtained by fixing  $N_*$  in the values  $N_* = 50$  (upper curve) and  $N_* = 60$  (lower curve).

for the E model ( $n = 1$ ), we have that

$$\begin{aligned} \phi_*^{n=1} = & \sqrt{\frac{3\alpha}{\pi}} \frac{m_{\text{Pl}}}{4} \left\{ \frac{1 + 2\text{arccoth}(a_1)}{a_1 - 1} \right. \\ & - W_{-1} \left[ \frac{e^{-1 + \frac{2}{a_1 - 1} - \frac{4N_*}{3\alpha}} (1 + a_1)}{a_1 - 1} \right] \\ & - \frac{4N_*}{3(a_1 - 1)\alpha} \\ & \left. + \frac{a_1}{a_1 - 1} \left( 1 - 2\text{arccoth}(a_1) + \frac{4N_*}{3\alpha} \right) \right\}, \end{aligned} \quad (5.9)$$

and for  $n = 2$ , we have that

$$\begin{aligned} \phi_*^{n=2} = & \frac{m_{\text{Pl}}}{24\sqrt{\pi\alpha}} \left\{ -12\sqrt{\alpha} - 16\sqrt{3}N_* \right. \\ & + 3\sqrt{3}\alpha (-1 + 4\text{arccoth}(a_2)) \\ & \left. - W_{-1} \left[ -e^{-1 - \frac{4}{\sqrt{3}\sqrt{\alpha}} + 4\text{arccoth}(a_2) - \frac{16N_*}{3\alpha}} \right] \right\} \end{aligned} \quad (5.10)$$

where in the above equations,  $W_{-1}(x)$  is the Lambert function.

Note that the above equations depend on the value of  $\alpha$ . In Fig. 5 we show the potential normalization  $V_0$  as a function of  $\alpha$  when making use of Eq. (5.2).

The use of the tensor-to-scalar ratio  $r$  and the spectral tilt  $n_s$  of the scalar spectrum allows us to find an upper bound for the parameter  $\alpha$  for each of the potentials considered here.  $r$  and  $n_s$  are defined by [66]

$$r = 16\epsilon_V, \quad (5.11)$$

and

$$n_s = 1 - 6\epsilon_V + 2\eta_V, \quad (5.12)$$

where  $\epsilon_V$  and  $\eta_V$  are the slow-roll coefficients:

$$\epsilon_V = \frac{m_{\text{Pl}}^2}{16\pi} \left( \frac{V'}{V} \right)^2, \quad \eta_V = \frac{m_{\text{Pl}}^2}{8\pi} \frac{V''}{V}, \quad (5.13)$$

and which are evaluated at the value  $\phi_*$ .

From the expressions (5.8) – (5.10), we evaluate both  $r$  and  $n_s$  for the fiducial values of  $N_* = 50$  and  $N_* = 60$  as a function of  $\alpha$ . The results are shown in Fig. 6. For  $\alpha \ll 1$ , the results approach the ones given in Eqs. (2.3) and (2.2), for  $r$  and  $n_s$ , respectively. For  $\alpha > 1$ , the tensor-to-scalar ratio gives the stronger constrain on the value for  $\alpha$  for each type of potential, leading to the values given in Eq. (2.6).

- 
- [1] A. Ashtekar and J. Lewandowski, Background independent quantum gravity: A status report, *Classical Quantum Gravity* **21**, R53 (2004).
- [2] A. Ashtekar and P. Singh, Loop quantum cosmology: A status report, *Classical Quantum Gravity* **28**, 213001 (2011).
- [3] C. Rovelli and F. Vidotto, *Covariant Loop Quantum Gravity: An Elementary Introduction to Quantum Gravity and Spinfoam Theory* (Cambridge University Press, Cambridge, England, 2014).
- [4] A. Ashtekar, M. Bojowald, and J. Lewandowski, Mathematical structure of loop quantum cosmology, *Adv. Theor. Math. Phys.* **7**, 233 (2003).
- [5] M. Bojowald, Loop quantum cosmology, *Living Rev. Relativity* **8**, 11 (2005).
- [6] A. Ashtekar, T. Pawłowski, and P. Singh, Quantum nature of the big bang, *Phys. Rev. Lett.* **96**, 141301 (2006).
- [7] A. Ashtekar and D. Sloan, Loop quantum cosmology and slow roll inflation, *Phys. Lett. B* **694**, 108 (2011).
- [8] A. Barrau, T. Cailleteau, J. Grain, and J. Mielczarek, Observational issues in loop quantum cosmology, *Classical Quantum Gravity* **31**, 053001 (2014).
- [9] I. Agullo and P. Singh, Loop quantum cosmology, *100 Years of General Relativity* (World Scientific, Singapore, 2017).
- [10] T. Zhu, A. Wang, G. Cleaver, K. Kirsten and Q. Sheng, Pre-inflationary universe in loop quantum cosmology, *Phys. Rev. D* **96**, 083520 (2017).
- [11] M. Shahalam, M. Sharma, Q. Wu, and A. Wang, Preinflationary dynamics in loop quantum cosmology: Power-

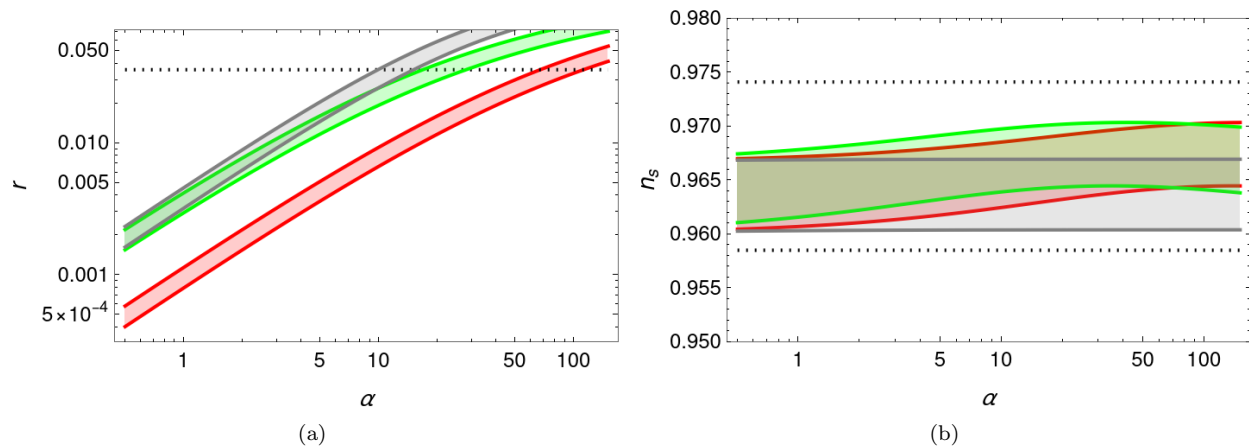


FIG. 6. The tensor-to-scalar ratio (a) and the spectral tilt (b) for the  $\alpha$ -attractor potential models considered in this work. The gray, green, and red curves and respective regions are for the T-model ( $n = 0$ ), E-model ( $n = 1$ ), and  $n = 2$   $\alpha$ -attractor models, respectively. The upper curves correspond to  $N_* = 50$ , while the lower curves are for  $N_* = 60$ . The horizontal dotted lines mark the upper bound for  $r$  [given by Eq. (2.5)] and the upper and lower ranges at  $2\text{-}\sigma$  for  $n_s$ .

- law potentials, Phys. Rev. D **96**, 123533 (2017).
- [12] B. F. Li, P. Singh, and A. Wang, Qualitative dynamics and inflationary attractors in loop cosmology, Phys. Rev. D **98**, 066016 (2018).
- [13] M. Sharma, M. Shahalam, Q. Wu, and A. Wang, Preinflationary dynamics in loop quantum cosmology: Monodromy Potential, J. Cosmol. Astropart. Phys. **11** (2018) 003.
- [14] B. F. Li, P. Singh, and A. Wang, Genericness of preinflationary dynamics and probability of the desired slow-roll inflation in modified loop quantum cosmologies, Phys. Rev. D **100**, 063513 (2019).
- [15] M. Shahalam, M. Al Ajmi, R. Myrzakulov, and A. Wang, Revisiting pre-inflationary Universe of family of  $\alpha$ -attractor in loop quantum cosmology, Classical Quantum Gravity **37**, 195026 (2020).
- [16] A. Ashtekar and D. Sloan, Probability of inflation in loop quantum cosmology, Gen. Relativ. Gravit. **43**, 3619 (2011).
- [17] L. L. Graef and R. O. Ramos, Probability of warm inflation in loop quantum cosmology, Phys. Rev. D **98**, 023531 (2018).
- [18] L. Linsefors and A. Barrau, Duration of inflation and conditions at the bounce as a prediction of effective isotropic loop quantum cosmology, Phys. Rev. D **87**, 123509 (2013).
- [19] L. Linsefors and A. Barrau, Exhaustive investigation of the duration of inflation in effective anisotropic loop quantum cosmology, Classical Quantum Gravity **32**, 035010 (2015).
- [20] B. Bolliet, A. Barrau, K. Martineau, and F. Moulin, Some clarifications on the duration of inflation in loop quantum cosmology, Classical Quantum Gravity **34**, 145003 (2017).
- [21] K. Martineau, A. Barrau, and S. Schander, Detailed investigation of the duration of inflation in loop quantum cosmology for a Bianchi-I universe with different inflation potentials and initial conditions, Phys. Rev. D **95**, 083507 (2017).
- [22] L. N. Barboza, L. L. Graef, and R. O. Ramos, Warm bounce in loop quantum cosmology and the prediction for the duration of inflation, Phys. Rev. D **102**, 103521 (2020).
- [23] L. N. Barboza, G. L. L. W. Levy, L. L. Graef, and R. O. Ramos, Constraining the Barbero-Immirzi parameter from the duration of inflation in loop quantum cosmology, Phys. Rev. D **106**, 103535 (2022).
- [24] R. Kallosh and A. Linde, Universality class in conformal inflation, J. Cosmol. Astropart. Phys. **07** (2013) 002.
- [25] R. Kallosh, A. Linde, and D. Roest, Superconformal inflationary  $\alpha$  attractors, J. High Energy Phys. **11** (2013) 198.
- [26] R. Kallosh, A. Linde, and D. Roest, Universal attractor for inflation at strong coupling, Phys. Rev. Lett. **112**, 011303 (2014).
- [27] M. Shahalam, M. Sami, and A. Wang, Preinflationary dynamics of  $\alpha$ -attractor in loop quantum cosmology, Phys. Rev. D **98**, 043524 (2018).
- [28] A. Dapor and K. Liegener, Cosmological effective Hamiltonian from full loop quantum gravity dynamics, Phys. Lett. B **785**, 506 (2018).
- [29] I. Agullo, Primordial power spectrum from the Dapor-Liegener model of loop quantum cosmology, Gen. Relativ. Gravit. **50**, 91 (2018).
- [30] E. Alesci, G. Botta, F. Cianfrani, and S. Liberati, Cosmological singularity resolution from quantum gravity: The emergent-bouncing universe, Phys. Rev. D **96**, 046008 (2017).
- [31] J. Olmedo and E. Alesci, Power spectrum of primordial perturbations for an emergent universe in quantum reduced loop gravity, J. Cosmol. Astropart. Phys. **04** (2019) 030.
- [32] Y. Akrami *et al.* (Planck Collaboration), Planck 2018 results. X. Constraints on inflation, Astron. Astrophys. **641**, A10 (2020).
- [33] N. Aghanim *et al.* (Planck Collaboration), Planck 2018 results. V. CMB power spectra and likelihoods, Astron. Astrophys. **641**, A5 (2020).
- [34] A. A. Starobinsky, A new type of isotropic cosmological models without singularity, Phys. Lett. B **91**, 99 (1980).

- [35] E. V. Linder, Dark energy from  $\alpha$  attractors, *Phys. Rev. D* **91**, 123012 (2015).
- [36] M. Shahalam, R. Myrzakulov, S. Myrzakul, and A. Wang, Observational constraints on the generalized  $\alpha$  attractor model, *Int. J. Mod. Phys. D* **27**, 1850058 (2018).
- [37] D. I. Kaiser and E. I. Sfakianakis, Multifield inflation after Planck: The case for nonminimal couplings, *Phys. Rev. Lett.* **112**, 011302 (2014).
- [38] R. Kallosh, A. Linde, and D. Roest, Large field inflation and double  $\alpha$ -attractors, *J. High Energy Phys.* 08 (2014) 052.
- [39] K. Dimopoulos and C. Owen, Quintessential inflation with  $\alpha$ -attractors, *J. Cosmol. Astropart. Phys.* 06 (2017) 027.
- [40] J. J. M. Carrasco, R. Kallosh, and A. Linde,  $\alpha$  attractors: Planck, LHC and dark energy, *J. High Energy Phys.* 10 (2015) 147.
- [41] A. R. Liddle and S. M. Leach, How long before the end of inflation were observable perturbations produced?, *Phys. Rev. D* **68**, 103503 (2003).
- [42] P. A. R. Ade *et al.* (BICEP and Keck Collaborations), Improved constraints on primordial gravitational waves using Planck, WMAP, and BICEP/Keck observations through the 2018 observing season, *Phys. Rev. Lett.* **127**, 151301 (2021).
- [43] K. A. Meissner, Black hole entropy in loop quantum gravity, *Classical Quantum Gravity* **21**, 5245 (2004).
- [44] J. Engle, K. Noui, A. Perez, and D. Pranzetti, Black hole entropy from an SU(2)-invariant formulation of Type I isolated horizons, *Phys. Rev. D* **82**, 044050 (2010).
- [45] E. Bianchi, Entropy of non-extremal black holes from loop gravity, arXiv:1204.5122.
- [46] P. J. Wong, Shape dynamical loop gravity from a conformal Immirzi parameter, *Int. J. Mod. Phys. D* **26**, 1750131 (2017).
- [47] I. Agullo, A. Ashtekar, and W. Nelson, A quantum gravity extension of the inflationary scenario, *Phys. Rev. Lett.* **109**, 251301 (2012).
- [48] M. Benetti, L. Graef, and R. O. Ramos, Observational constraints on warm inflation in loop quantum cosmology, *J. Cosmol. Astropart. Phys.* 10 (2019) 066.
- [49] M. Fernandez-Mendez, G. A. Mena Marugan, and J. Olmedo, Hybrid quantization of an inflationary universe, *Phys. Rev. D* **86**, 024003 (2012).
- [50] B. F. Li, J. Olmedo, P. Singh, and A. Wang, Primordial scalar power spectrum from the hybrid approach in loop cosmologies, *Phys. Rev. D* **102**, 126025 (2020).
- [51] A. Ashtekar and B. Gupta, Initial conditions for cosmological perturbations, *Classical Quantum Gravity* **34**, 035004 (2017).
- [52] D. M. de Blas and J. Olmedo, Primordial power spectra for scalar perturbations in loop quantum cosmology, *J. Cosmol. Astropart. Phys.* 06 (2016) 029.
- [53] M. Martín-Benito, R. B. Neves, and J. Olmedo, States of low energy in bouncing inflationary scenarios in loop quantum cosmology, *Phys. Rev. D* **103**, 123524 (2021).
- [54] L. J. Garay, M. L. González, M. Martín-Benito, and R. B. Neves, An adiabatic approach to the trans-Planckian problem in Loop Quantum Cosmology, *Phys. Rev. D* **109**, 123534 (2024).
- [55] J. Martin and R. H. Brandenberger, The trans-Planckian problem of inflationary cosmology, *Phys. Rev. D* **63**, 123501 (2001).
- [56] R. H. Brandenberger and J. Martin, Trans-Planckian issues for inflationary cosmology, *Classical Quantum Gravity* **30**, 113001 (2013).
- [57] A. Bedroya and C. Vafa, Trans-Planckian censorship and the swampland, *J. High Energy Phys.* 09 (2020) 123.
- [58] A. Bedroya, R. Brandenberger, M. Loverde, and C. Vafa, Trans-Planckian censorship and inflationary cosmology, *Phys. Rev. D* **101**, 103502 (2020).
- [59] A. H. Guth, Inflation and eternal inflation, *Phys. Rep.* **333**, 555 (2000).
- [60] P. W. Graham, D. E. Kaplan, and S. Rajendran, Cosmological relaxation of the electroweak scale, *Phys. Rev. Lett.* **115**, 221801 (2015).
- [61] P. W. Graham and A. Scherlis, Stochastic axion scenario, *Phys. Rev. D* **98**, 035017 (2018).
- [62] S. Y. Ho, F. Takahashi, and W. Yin, Relaxing the cosmological moduli problem by low-scale inflation, *J. High Energy Phys.* 04 (2019) 149.
- [63] F. Takahashi and W. Yin, QCD axion on hilltop by a phase shift of  $\pi$ , *J. High Energy Phys.* 10 (2019) 120.
- [64] C. Ringeval, T. Suyama, T. Takahashi, M. Yamaguchi, and S. Yokoyama, Dark energy from primordial inflationary quantum fluctuations, *Phys. Rev. Lett.* **105**, 121301 (2010).
- [65] C. Ringeval, T. Suyama, and M. Yamaguchi, Large mass hierarchy from a small nonminimal coupling, *Phys. Rev. D* **99**, 123524 (2019).
- [66] D. H. Lyth and A. R. Liddle, *The Primordial Density Perturbation: Cosmology, Inflation and the Origin of Structure* (Cambridge University Press, Cambridge, England, 2009).
- [67] N. Aghanim *et al.* (Planck Collaboration), Planck 2018 results. VI. Cosmological parameters, *Astron. Astrophys.* **641**, A6 (2020); **652**, C4(E) (2021).